Composites Part B 207 (2021) 108601

Contents lists available at ScienceDirect

Composites Part B

journal homepage: www.elsevier.com/locate/compositesb

A highly fire-safe and smoke-suppressive single-component epoxy resin with switchable curing temperature and rapid curing rate

Shuang Yang [a,c], Siqi Huo [b,e,*], Jun Wang [c,d], Bin Zhang [d], Jingsheng Wang [d], Shiya Ran [b], Zhengping Fang [b], Pingan Song [e,**], Hao Wang [e]

[a] School of Mechanical and Electronic Engineering, Wuhan University of Technology, Wuhan, 430070, China
[b] Laboratory of Polymer Materials and Engineering, NingboTech University, Ningbo, 315100, China
[c] Institute of Advanced Material Manufacturing Equipment and Technology, Wuhan University of Technology, Wuhan, 430070, China
[d] School of Materials Science and Engineering, Wuhan University of Technology, Wuhan, 430070, China
[e] Centre for Future Materials, University of Southern Queensland, Toowoomba, QLD, 4350, Australia

ARTICLE INFO

Keywords:
Single-component epoxy resin
Benzimidazole
Curing behaviors
Fire retardancy
Smoke suppression

ABSTRACT

The design of highly fire-safe and smoke-suppressive single-component epoxy (EP) resins combining modest curing temperature and fast curing rate has been desirable yet very challenging in both academia and industry. Herein, we report a facile design of a phosphorus/imidazole-containing single-component EP system *via* incorporating 9,10-dihydro-9-oxa-10-phosphaphenanthrene-10-oxide (DOPO) and a flame-retardant curing agent cyclotriphosphazene-modified benzimidazole (BICP) into EP. Our results show that EP/DOPO/BICP exhibits a rapid modest-temperature curing feature because DOPO serves as a switch that triggers BICP to release benzimidazole (BIM) *via* substitution reaction in the initial curing stage. Moreover, as-prepared EP/DOPO/BICP shows outstanding fire retardancy, reflected by the high limited oxygen index (LOI) of 38.3% and UL-94 V-0 rating. Compared to the control EP system, the peak of heat release rate (PHRR) and total smoke production (TSP) of EP/DOPO/BICP remarkably decrease by ~74.5% and ~50.6%, respectively, which is superior to previously-reported flame-retardant P-containing epoxy counterparts. The significant enhancements in flame retardancy and smoke suppression are mainly due to the formation of a highly intumescent char layer and the reduced burning degree of pyrolysis fragments. This work offers a facile and scalable strategy for creating fast-curing, modest-temperature curable, highly fire-resistant and smoke-suppressive one-component epoxy systems applicable to large-scale industrial production.

1. Introduction

Polymers have already been ubiquitous in modern society since their discovery [1–3]. As one class of important thermoset polymers, epoxy resins (EPs) are extensively applied in construction, automotive, electronics and aerospace areas because of high mechanical strength, outstanding adhesion, chemical resistance, and good electrical insulation [4–6]. Generally, the epoxy resin can be cured by a variety of curing agents (e.g., amine, phenol, anhydride and imidazole), under a specific condition [7–10]. Among these curing agents, imidazole has recently attracted particular interests because it can rapidly cure EPs *via* inducing the anionic chain polymerization of epoxy groups in the resin. For this reason, imidazole and its derivatives are widely employed as thermal latent curing agents to fabricate single-component epoxy systems, which is beneficial to reducing environmental pollution and meeting the requirements of large-scale industrial production [11,12].

However, unmodified imidazoles suffer extremely high activity, which are capable of curing epoxy resins within one or two days even at room temperature, leading to short shelf life and poor storage stability [13,14]. To lower the activity, different functional groups have been introduced into 1-position and 3-position nitrogen atoms of the imidazole ring. For instance, Wei et al. synthesized an imidazole-copper (II) complex as a thermal latent curing agent for EP [11]. The incorporation of copper (II) significantly improves the storage stability of the as-prepared single-component EP, which can be stored at room temperature for 8 days. Arimitsu et al. reported three similar imidazole

* Corresponding author. Laboratory of Polymer Materials and Engineering, NingboTech University, Ningbo, 315100, China.
** Corresponding author.
E-mail addresses: sqhuo@hotmail.com (S. Huo), pingansong@gmail.com (P. Song).

https://doi.org/10.1016/j.compositesb.2020.108601
Received 31 October 2020; Received in revised form 13 December 2020; Accepted 22 December 2020
Available online 25 December 2020

derivatives containing long-chain alkyl succinate group [15], which exhibited high curability towards epoxy resin at ~120 °C. As a result, the resultant EP systems show a long shelf life of more than 12 days at ambient temperature. These attempts have fully shown that introducing functional groups with electron-withdrawing inductive or steric hindrance effect can effectively enhance the thermal latency of imidazole-derived curing agents for EPs.

In addition, intrinsic flammability is another major issue of common EPs, which limits their practical applications in many industrial areas with high fire safety requirements [16–19]. To address this issue, many kinds of phosphorus-containing compounds, such as phosphaphenanthrene, phosphate and cyclotriphosphazene, have been explored to prepare flame retardant EPs due to their high flame retardant efficacy and low toxicity [20–23]. For this reason, several phosphorus-modified imidazole derivatives have been developed to combine fast curing rate and great flame retardancy characteristics [24–26]. For example, Wang et al. developed a phosphorus-containing imidazolium (IDPP) for fabricating one-component flame retardant EP [10]. As-fabricated epoxy thermoset features outstanding flame retardancy, showing a LOI and UL-94 rating of 37.0% and V-0, respectively. Previously, we also reported a cyclotriphosphazene-containing benzimidazole derivative (BICP) as flame-retardant thermal latent curing agent for EPs [27]. With the inclusion of cyclotriphosphazene group, the final epoxy thermoset shows enhanced flame retardancy, e.g., a LOI value of 33.5% and a UL-94 V-0 rating. Despite this, differential scanning calorimetry (DSC) analyses show that the curing temperatures of EP/BICPs are very high, with their peak curing temperatures up to ~210 °C, ultimately restricting their practical applications in industry. In addition to flame retardancy, smoke suppression is another important parameter to evaluate the fire safety of polymeric materials because most fire deaths are caused by inhalation of smoke [9,28,29]. Nevertheless, a large amount of smoke is generated during the combustion of EP/BICPs, as also reported in other EP/P-containing imidazole systems [10,25,30]. Given high fire resistance efficiency of cyclotriphosphazene and phosphaphenanthrene groups [31–33], it is possible to develop flame-retardant and smoke-suppressive EPs by combining DOPO and BICP. Additionally, the imidazole-modified phosphazene compounds exhibit unique degradation behaviors in basic media, which will decompose to release imidazole molecules during decomposition [34,35].

This work aims to develop a single-component EP system with excellent flame retardancy and smoke suppression by directly adding DOPO into EP/BICP. As expected, our results show that the presence of DOPO significantly reduces the peak curing temperature of EP/DOPO/BICP by about 30 °C, enabling the EP/DOPO/BICP to completely cure within 7 min at 180 °C. This is because DOPO serves as a switch that reacts with BICP *via* nucleophilic substitution to facilitate the generation of BIM at the initial curing stage (see Scheme 1). Besides retaining high glass transition temperature, the ternary EP/DOPO/BICP system shows ~74.5% and ~50.6% reductions in PHRR and TSP relative to those of the unmodified binary EP/BIM, respectively, which are superior to many previous works. Therefore, this work offers a feasible strategy for massively creating flame-retardant and smoke-suppressive one-component epoxy systems with switchable curing temperature and rapid curing rate, thus holding great promise for practical applications in electrical, auto, aerospace, etc.

2. Experimental section

2.1. Materials

Diglycidyl ether of bisphenol-A (DGEBA, epoxide equivalent weight: ~188 g/equiv) was purchased from Yueyang Baling Huaxing Petrochemical Co., Ltd (Hunan, China). DOPO was purchased from Huizhou Sunstar Technology Co., Ltd (Guangdong, China). Benzimidazole (BIM) was supplied by Aladdin Industrial Co., Ltd (Shanghai, China). BICP was synthesized according to our previous work [27]. All other commercially available reagents were used as received.

2.2. Fabrication of EP thermosets

100 g DGEBA and 10 g DOPO were blended at 120 °C for 30 min to form a transparent solution. A certain amount of BICP was introduced into the solution when cooled to 90 °C, and the mixture was stirred at

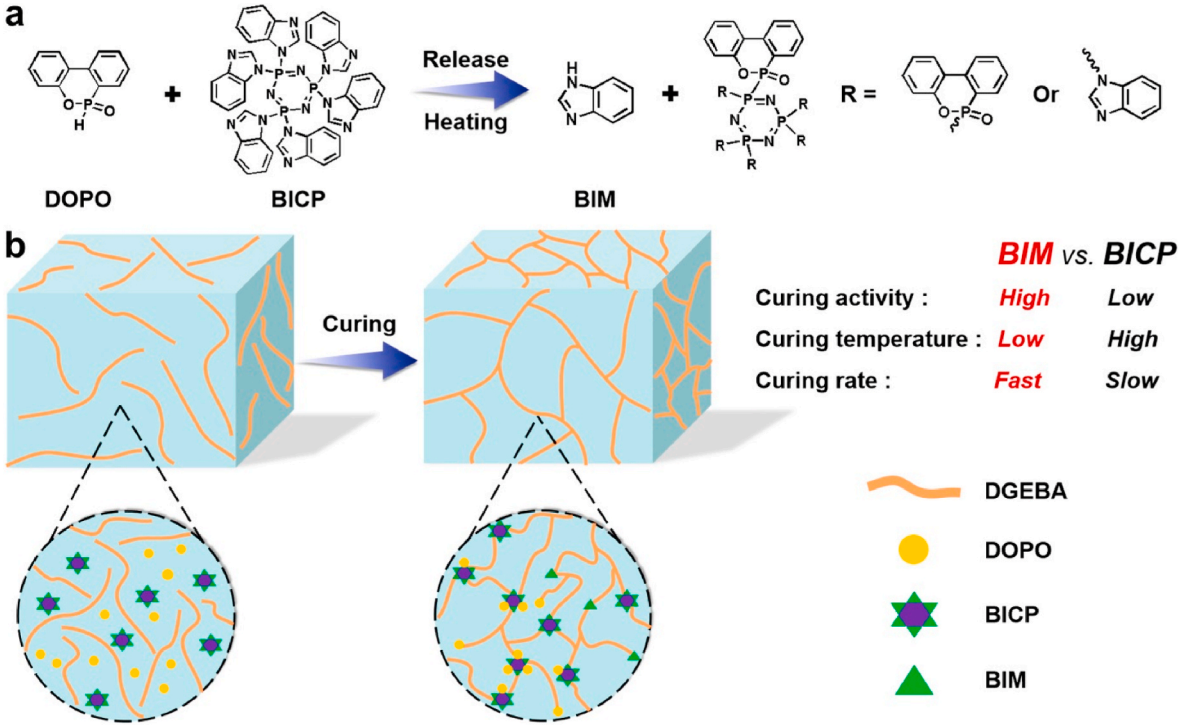

Scheme 1. (a) Proposed nucleophilic substitution reaction of DOPO and BICP, and (b) curing process of EP/DOPO/BICP.

90 °C until it became transparent. A small quantity of the mixture was reserved for differential scanning calorimetry (DSC) tests. The mixture was degassed under vacuum, and poured into a preheated mold in an oven. The target EP/DOPO/BICP samples were obtained by curing at 130 °C for 1 h and then 170 °C for 2 h, respectively. Both EP/BIM-10 and EP/BICP-12 samples are also prepared according to our previous work [27]. The formulas of these EP samples are listed in Table 1.

2.3. Characterizations

Pyrolysis-gas chromatography/mass spectrometry (Py-GC/MS) was conducted on an Agilent 7890/5975 GC/MS (Agilent, US) combined with a CDS5000 pyrolizer (CDS, US) with the pyrolysis temperature of 140 °C. X-ray photoelectron spectroscopy (XPS) measurement was undertaken on an ESCALAB 250 X-ray photoelectron spectrometer (VG Scientific, UK) with Al Kα excitation radiation. Differential scanning calorimetry (DSC) was undertaken on a Perkin-Elmer DSC 4000 (PerkinElmer, US) under N_2 conditions at a heating rate of 10 °C/min. Viscosity values of EP mixtures at room temperature were recorded on ARES dynamic rotational rheometer (TA, US).

Thermogravimetric analysis (TGA) was conducted using a NETZSCH STA449F3 (NETZSCH-Gerätebau GmbH, Germany) at a heating rate of 10 °C/min from 40 to 800 °C under nitrogen atmosphere. Dynamic mechanical analysis (DMA) was performed on a DMA Q 800 apparatus (TA, US) (constant frequency = 1.0 Hz, 30–250 °C, heating rate = 5 °C/min) in a three-point bending model with the specimen dimension of 20 × 1 × 4 mm^3.

Limited oxygen index (LOI) was obtained by a JF-3 oxygen index meter (Jiangning Analysis Instrument Company, China) according to ASTM D2863, with specimen dimensions of 130 × 6.5 × 3 mm^3. Vertical burning (UL-94) grade was measured on a NK8017A instrument (Nklsky Instrument Co., Ltd., China) according to ASTM D 63577, with sheet dimension of 130 × 13 × 3.0 mm^3. Cone calorimeter tests were conducted on an FTT cone calorimeter (Fire Testing Technology, East Grinstead, UK) according to ISO 5660 under a heat flux of 50 kW/m^2. The sample dimension was 100 × 100 × 3.0 mm^3. Typically, three specimens for each sample were tested, and the error values of the obtained data were reproducible within ±5%.

Thermogravimetric analysis/infrared spectrometry (TG-IR) was conducted on a Q5000IR thermo-analyzer (TA, US) integrated with a Nicolet 6700 infrared spectrometer (Thermo Fisher Scientific, US) with a heating rate of 20 °C/min. About 8.0–10.0 mg of powder sample was heated from 30 to 800 °C under N_2 flow. QuantaFEG450 (FEI, US) scanning electron microscope (SEM) was applied to investigate the micro morphology of char layers generated by cone calorimeter tests. SEM was integrated with an energy dispersive spectrometer (EDS) microanalyzer for the analysis of the elemental compositions. Raman spectra were recorded on a Renishaw Invia Raman Microscope (Renishaw, UK) using a 532 nm argon ion laser.

Table 1
The formulas of EP thermosets.

Sample code	DGEBA (g)	BIM (g)	DOPO (g)	BICP (g)	P content (wt %)
EP/BIM-10	100	10	/	/	/
EP/BICP-12	100	/	/	12	1.2
EP/DOPO/BICP-7	100	/	10	7.7	1.9
EP/DOPO/BICP-11	100	/	10	12.1	2.3
EP/DOPO/BICP-15	100	/	10	16.5	2.6

3. Results and discussion

3.1. Curing behaviors and storage stability

Similar to other imidazole-containing phosphazene analogs, BICP may decompose to release benzimidazole molecules with high curing activity. DOPO, as a Lewis base, is expected to trigger BICP to release benzimidazole molecules under heating. Thus, the Py-GC/MS and XPS measurements of DOPO and BICP mixture (mass ratio: 1:1) were conducted to investigate the molecular change of DOPO and BICP mixture. For Py-GC/MS, we intentionally set the pyrolysis temperature at 140 °C to make it over the melting point of DOPO, while at which BICP was thermally stable [27]. The DOPO and BICP mixture for XPS measurement was placed at 140 °C for 30 min in advance. As shown in Fig. 1a, abundant benzimidazole molecules (m/z = 118) are detected at a retention time of about 15 min during Py-GC/MS measurement, demonstrating the trigger effect of DOPO. The high-resolution P2p XPS spectrum (see Fig. 1b) can be deconvoluted into four peaks at 130.1, 131.1, 132.2, and 133.4 eV, corresponding to $P2p_{3/2}$ and $P2p_{1/2}$ of P–P, P–O–C and P–N bonds [23,36], respectively, indicating that DOPO connects with the cyclotriphosphazene of BICP *via* P–P bonds. As presented in Fig. S2 (Supporting information), the N1s peak at 399.7 eV can be attributed to C–N–H bonds [36], further confirming the generation of benzimidazole molecules. These fully indicate that DOPO can serve as a switch under heating, and trigger BICP to release benzimidazole molecules *via* nucleophilic substitution reaction to rapidly cure the EP. Similar decomposition behaviors have also been previously reported in imidazole-modified phosphazene systems [34,35].

Based on the above results, DOPO is introduced into EP/BICP system to lower the curing temperature. The curing behaviors of EP/BIM-10, EP/BICP-12, and EP-DOPO/BICP mixtures were investigated by DSC measurements, with non-isothermal and isothermal curves presented in Fig. 1c and d, and characteristic curing data listed in Table 2. The EP/DOPO/BICPs clearly show two exothermic curing peaks located at ~168 °C and ~183 °C (see Fig. 1c and Table 2), respectively. The first curing peak is attributed to the addition reaction between DOPO and epoxy groups [37], whereas the second peak is assigned to the polymerization of epoxy groups initiated by imidazole rings. As expected, the polymerization peaks of the EP/DOPO/BICPs significantly shift to lower temperatures relative to the EP/BICP-12. For instance, EP/DOPO/BICP-11 exhibits a T_o of 151 °C and a $T_{P,2}$ of 183 °C, which are respectively 41 °C and 28 °C lower than 192 °C and 211 °C of the EP/BICP-12. The reduced curing temperature is further confirmed by the isothermal curves of the EP/DOPO/BICP-11 (see Fig. 1d). The polymerization can be initiated at only 120 °C, and the exothermic curing peak becomes increasingly obvious as the temperature increases. In addition, only 53.4% of epoxy groups in the EP/BICP-12 are consumed within 32.6 min at 150 °C in comparison to a 60.5% consumption of epoxy groups in the EP/DOPO/BICP-11 within 25.3 min at 140 °C (see Fig. 1e). When the curing temperature increases to 180 °C, the EP/DOPO/BICP-11 cures rapidly, exhibiting a complete consumption of epoxy groups within 7 min. The results clearly indicate that the presence of DOPO can strikingly promote the curing of the EP/BICP, giving rise to reduced curing temperatures.

Given the above results, it is reasonable to propose three possible curing reactions during the curing of the EP/DOPO/BICPs, as illustrated in Scheme 2. Firstly, DOPO reacts with epoxy groups in DGEBA (see Scheme 2a). Secondly, DOPO prompts BICP to release benzimidazole molecules that then induce the chain polymerization of epoxy resin (see Scheme 2c). Thirdly, the undecomposed and partially decomposed BICP molecules also induce chain polymerization of the epoxy resin (see Scheme 2b).

In addition, the storage stability of EP/BIM-10 and EP/DOPO/BICP-11 was evaluated *via* testing their viscosity changes as a function of time at room temperature. Generally, the shelf life of one-component EP is defined as the time required for the normalized viscosity to double in

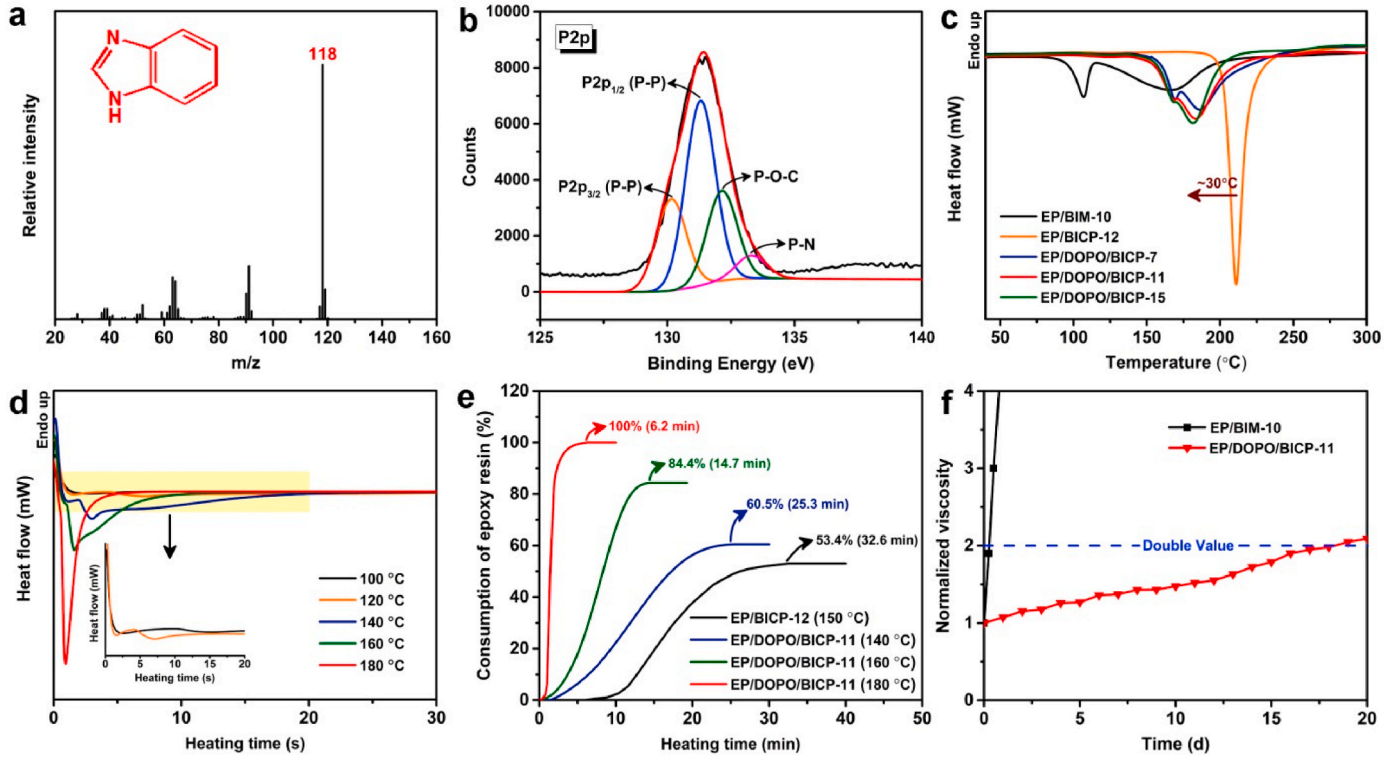

Fig. 1. (a) Py-GC/MS spectrum of BICP and DOPO mixture (Pyrolysis temperature: 140 °C, and retention time: ~15 min), (b) high-resolution P2p spectrum of the pre-heated BICP and DOPO mixture, (c) non-isothermal DSC curves of EP/BIM-10, EP/BICP-12 and EP/DOPO/BICPs, (d) isothermal DSC curves of EP/DOPO/BICP-11, (e) consumption of epoxy resins in isothermal DSC analyses, and (f) viscosity verses time curves of EP/BIM-10 and EP/DOPO/BICP-11.

Table 2
DSC data of EP mixtures.

Sample code	T_o[a] (°C)	$T_{p,1}$[a] (°C)	$T_{p,2}$[a] (°C)	T_t[a] (°C)	ΔH[a] (J/g)
EP/BIM-10	95	106	166	204	470
EP/BICP-12	192	211	/	236	535
EP/DOPO/BICP-7	153	169	186	215	453
EP/DOPO/BICP-11	151	168	183	206	469
EP/DOPO/BICP-15	153	168	181	202	494

[a] T_o: onset curing temperature; $T_{p,1}$: the first peak curing temperature; $T_{p,2}$: the second peak curing temperature; T_t: terminal curing temperature; ΔH: total exothermic heat.

value [38]. Without modification, EP/BIM-10 suffers extremely high curing activity, and its solidification can be completed within 2 days (see Fig. 1f). In a sharp contrast, the EP/DOPO/BICP-11 shows significantly enhanced storage stability, as reflected by a shelf life as long as 20 days. The encouraging result demonstrates that the as-prepared EP/DOPO/-BICPs are very suitable to be developed as one-component epoxy resin for fiber-epoxy prepregs expecting to reduce environmental pollution and meet the requirements of massive industry production.

3.2. Thermal properties

The thermal properties of EP/BIM-10, EP/BICP-12 and EP/DOPO/BICPs were investigated by DMA and TGA techniques, with corresponding curves and data shown in Fig. 2 and Table 3. The T_g values of all of EP/DOPO/BICPs are lower than that of the EP/BICP-12 (see Fig. 2a) due to the end-capping reaction of EP and DOPO [37], but still much higher than that of the EP/BIM-10 because of the rigid structure of P-containing groups and polyfunctionality of the BICP. The high T_g values (>170 °C) of the EP/DOPO/BICPs clearly indicate their good thermal resistance, thus enabling them to find extensive applications in electronics, automotive and aerospace fields. Additionally, the incorporation of rigid DOPO increases the E' values to some extent (see Fig. 2b), demonstrating the improved stiffness of the EP/DOPO/BICPs.

The TG and DTG curves of EP/BIM-10, EP/BICP-12 and EP/DOPO/BICPs are presented in Fig. 2c and d, with characteristic parameters listed in Table 3. The introduction of DOPO and BICP gives rise to high P content. Therefore, the EP/DOPO/BICPs show lower $T_{5\%}$ and T_{max} values than those of EP/BIM-10 and EP/BICP-12 due to the catalytic decomposition effect of phosphorus [39]. The maximum weight loss rate (R_{max}) values of EP/DOPO/BICPs decrease gradually with the increasing P content. For example, the R_{max} value of EP/DOPO/BICP-15 decreases from 13.4%/min of EP/BIM-10 to 9.3%/min. This implies that the P-containing groups suppress the thermal decomposition of the EP matrix at high temperatures. Additionally, the char yields at 800 °C (*CY*s) of EP/DOPO/BICPs are much higher than that of the EP/BIM-10 and increase with the increase of BICP content, but lower than that of the EP/BICP-12 because DOPO mainly functions in the gas phase instead of the condensed phase [40,41].

3.3. Flame retardancy and smoke suppression

Both LOI and UL-94 measurements were used to evaluate the flame retardancy of EP/BIM-10, EP/BICP-12, and EP/DOPO/BICP samples, with the results listed in Table 4. Clearly, the control EP/BIM-10 sample is highly flammable, showing a low LOI value of 21.5%. Meanwhile, the sample cannot achieve any UL-94 rating and also suffers severe melt-dripping. For the EP/BICP system, the EP/BICP-12 sample with 1.2 wt % phosphorus exhibits the best flame retardancy with a high LOI value of 33.5% and a UL-94 V-0 rating [27]. In comparison, the inclusion of DOPO increases the P content, and as a result all the EP/DOPO/BICP samples exhibit higher LOI values than the EP/BICP-12 and acquire a UL-94 V-0 rating. These results fully indicate the improved flame retardancy of EP/DOPO/BICP samples due to the combination of phosphaphenanthrene and cyclotriphosphazene groups and higher P contents.

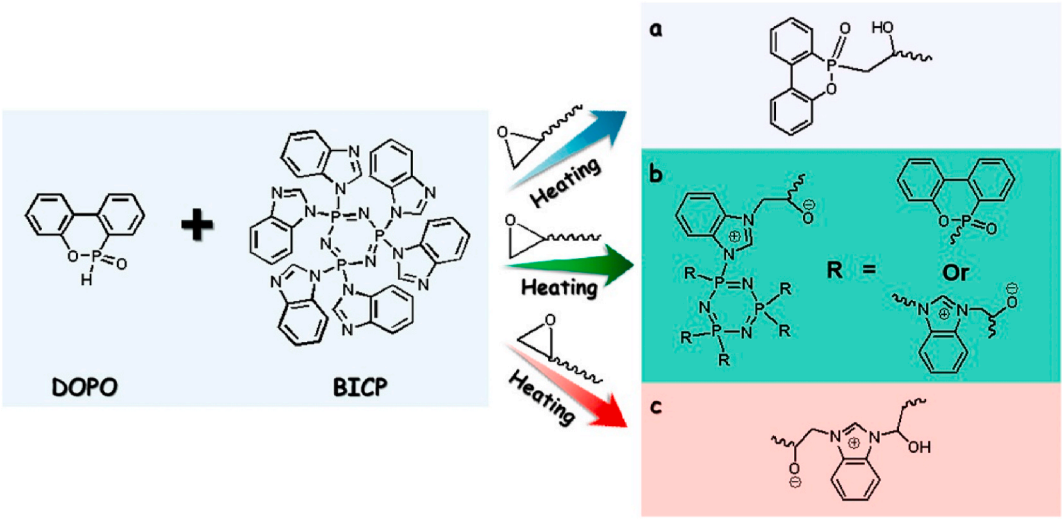

Scheme 2. (a) Addition reaction of DOPO and epoxy groups, the chain polymerization of epoxy resin induced by (b) the undecomposed and partially decomposed BICP, and (c) benzimidazole.

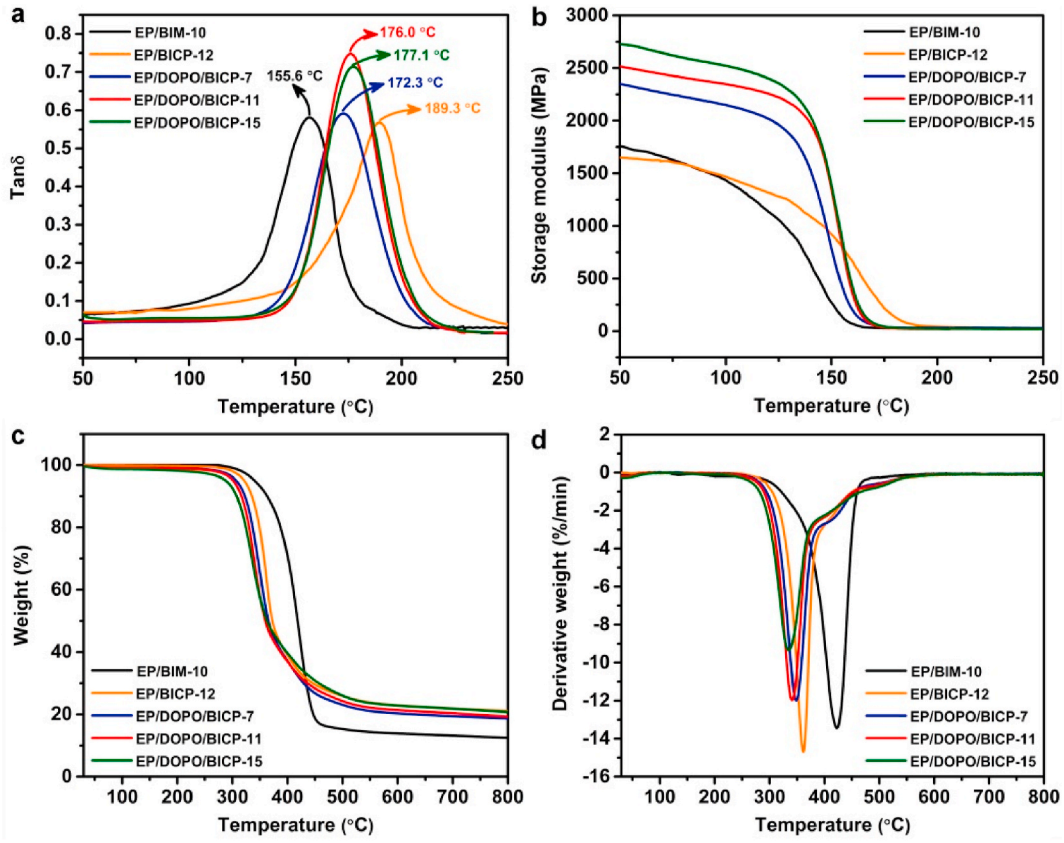

Fig. 2. (a) Tan delta, (b) storage modulus, (c) TG and (d) DTG curves *vs.* temperature curves of EP samples.

In addition, cone calorimeter tests are also employed to quantitatively assess the heat and smoke release of polymeric materials *via* simulating their combustion behavior in a real fire [9,25,42,43]. As presented in Table 4 and Fig. 3, without flame retardants, the EP/BIM-10 releases a large amount of heat during burning, with high PHRR and THR values of 1335 kW/m^2 and 95.0 MJ/m^2, respectively. Upon adding BICP or DOPO/BICP, both PHRR and THR values significantly reduce due to the incorporation of the element phosphorus. Especially, the EP/DOPO/BICP-11 with 2.3 wt% of phosphorus displays the lowest PHRR and THR values of 354 kW/m^2 and 44.8 MJ/m^2, respectively among all EPs, indicating superior flame retardancy, which is in good accordance with the LOI and UL-94 results. However, with the further increase in the BICP content, the PHRR and THR of EP/DOPO/BICP-15 increase instead. This is probably because the excess BICP results in deviation from the optimal ratio of phosphaphenanthrene and cyclotriphosphazene groups, thus leading to reduced flame retardancy, similar to previous reports [44,45]. In addition to PHRR and THR, the fire performance index (FPI) and fire growth rate (FGR) are

Table 3
DMA and TGA data of EP samples.

Sample code	T_g[a] (°C)	E'[a] (MPa)	ν_e[a] (mol/m^3)	$T_{5\%}$[a] (°C)	T_{max}[a] (°C)	R_{max}[a] (%/min)	CY[a] (%)
EP/BIM-10	155.6	1760	2237	342	420	13.4	12.5
EP/BICP-12	189.3	1650	2752	321	360	14.7	21.1
EP/DOPO/BICP-7	172.3	2351	2698	307	349	12.0	18.7
EP/DOPO/BICP-11	176.0	2515	1916	301	340	11.9	19.4
EP/DOPO/BICP-15	177.1	2727	2108	287	335	9.3	20.8

[a] T_g: glass transition temperature; E': storage modulus at 50 °C; ν_e: cross-linking density, which is calculated according to our previous work [27]; $T_{5\%}$: temperature at 5% weight loss; T_{max}: temperature at maximum weight loss rate; R_{max}: maximum weight loss rate; CY: char yield at 800 °C.

another two important parameters to evaluate the fire safety of materials. In general, the higher FPI value and the lower FGR value, the greater the flame retardancy [46,47]. As shown in Fig. 3c, the EP/DOPO/BICP-11 shows the highest FPI of 0.101 m^{2}s/kW and the lowest FGR of 2.6 kW/m^2/s, further demonstrating its greatest flame retardancy.

The smoke suppression has been identified as another crucial element of fire safety for materials because reported 60%–80% deaths in home fires are caused by smoke inhalation [48]. The total smoke production (TSP) and smoke production rate (SPR) curves are shown in Fig. 3d and e, with detailed data listed in Table 4. The EP/BICP-12 only shows a ~7.1% reduction in TSP relative to that of EP/BIM-10, indicating limited smoke suppression. Interestingly, the introduction of phosphaphenanthrene and cyclotriphosphazene groups leads to significant reductions in both TSP and PSPR values of EP/DOPO/BICPs. In particular, the TSP of EP/DOPO/BICP-11 decreases from 26.5 m^2 of EP/BIM-10 to 13.1 m^2 by ~50.6%, accompanied with a ~64.1% reduction in PSPR. The above results clearly show that EP/DOPO/BICP-11 features outstanding flame retardancy and smoke suppression.

To highlight the flame retardancy and smoke suppression of EP/DOPO/BICP-11, its PHRR and TSP reductions are compared with some previously-reported flame-retardant P-containing epoxy systems [6–10,16–18,49–54] (see Fig. 3f). Obviously, our EP/DOPO/BICP-11 exhibits greater reductions in both PHRR and TSP compared with other reported flame-retardant P-containing epoxy counterparts. This further manifests its unprecedented flame retardancy and smoke suppression due to the combination of phosphaphenanthrene and cyclotriphosphazene and high P content.

The average of effective heat of combustion (AEHC) reveals the burning degree of pyrolysis fragments in the gaseous phase [55,56]. To understand the flame-retardant gaseous-phase mechanism, the AEHC values of EP samples are listed in Table 4. The AEHC of EP/BICP-12 is close to that of EP/BIM-10, whereas those of EP/DOPO/BICPs significantly decrease by 24.0%–39.7%. This is because DOPO is featured by its prominent gaseous-phase flame-retardant effect by releasing P-based radicals (e.g., PO• and HPO) to scavenge unstable H• and OH• radicals during combustion [57–59]. Therefore, the declines in AEHC values of EP/DOPO/BICPs are mainly attributed to the introduction of DOPO. Regarding the residual weight at 500 s (RW) (see Table 4), both EP/BICP-12 and EP/DOPO/BICPs exhibit much higher RW values than the EP/BIM-10, but the RW values of all EP/DOPO/BICPs are close to that of EP/BICP-12, in good consistence with TGA results. These results indicate that the DOPO is ineffective in promoting the carbonization. In addition, the char residues of EP/DOPO/BICPs show highly intumescent structures (see Fig. 4), which contribute to suppressing the heat transfer and fuel supply. Hence, the superior fire safety of EP/DOPO/BICPs is mainly due to the significantly reduced burning degree of pyrolysis fragments in the gas phase and the formation of a highly intumescent char layer in the condensed phase.

3.4. TG-IR analyses of EPs

To further investigate the gas-phase mechanism, the TG-IR analyses of EP/BIM-10, EP/BICP-12 and EP/DOPO/BICP-11 under N_2 conditions were conducted. As shown in Fig. 5a–d, the typical decomposition gaseous products of EP thermoset are detected at 3720-3860 cm^{-1} (O–H), 2020-2230 cm^{-1} (carbon monoxide), 1730 cm^{-1} (C═O), 1530 cm^{-1} (benzene), and 1160 cm^{-1} (aliphatic compounds) [60,61]. Such results indicate the similar main decomposition products of EP/BIM-10, EP/BICP-12 and EP/DOPO/BICP-11. Notably, the incorporation of P-containing groups leads to decreased intensities of these peaks. In particular, EP/BICP-12 and EP/DOPO/BICP-11 exhibit reduced peak intensities of CO and C_{Ar}-C_{Ar} compared with EP/BIM-10 (see Fig. 5d and S3), and a similar trend can also be observed in the absorption peaks of hydrocarbons and carbonyl compounds (see Fig. 5e and f). In addition, the EP/DOPO/BICP-11 shows the lowest peak intensities (see Fig. 5e and f), further indicating the flame-retardant action of DOPO in the gaseous phase. As shown in Fig. 5i, in addition to the typical decomposition products, the absorption peaks of P═O, NH_2 and P–C appear at 1340, 978, 910 and 730 cm^{-1} [62,63] during the thermal decomposition of EP/DOPO/BICP-11. The generated ammonia can exert a diluting effect in the gas phase during combustion, and the P-containing fragments can further decompose to release PO• and HPO radicals to terminate the chain combustion reaction [64–66]. The TG-IR results further confirm

Table 4
The combustion data of EP samples.

Sample code	LOI (%)	UL-94 (3 mm)	PHRR[a] (kW/m^2)	THR[a] (MJ/m^2)	FPI[a] (m^{2}s/kW)	FGR[a] (kW/m^2/s)	TSP[a] (m^2)	PSPR[a] (m^2/s)	AEHC[a] (MJ/kg)	RW[a] (%)
EP/BIM-10	21.5	NR	1335 ± 20	95.0 ± 3.2	0.030 ± 0.001	12.4 ± 0.5	26.5 ± 1.0	0.348 ± 0.012	24.2 ± 0.3	3.9 ± 0.1
EP/BICP-12	33.5	V-0	403 ± 10	62.0 ± 1.5	0.072 ± 0.003	3.5 ± 0.2	24.4 ± 0.9	0.209 ± 0.008	23.8 ± 0.3	21.1 ± 0.4
EP/DOPO/BICP-7	34.2	V-0	403 ± 12	53.4 ± 1.8	0.097 ± 0.003	3.1 ± 0.2	16.7 ± 0.7	0.168 ± 0.006	16.0 ± 0.6	18.9 ± 0.5
EP/DOPO/BICP-11	38.3	V-0	354 ± 17	44.8 ± 1.9	0.101 ± 0.004	2.6 ± 0.1	13.1 ± 0.4	0.125 ± 0.004	14.6 ± 0.5	20.8 ± 0.8
EP/DOPO/BICP-15	36.1	V-0	389 ± 15	54.8 ± 1.7	0.085 ± 0.002	3.6 ± 0.1	15.9 ± 0.6	0.154 ± 0.007	18.4 ± 0.7	21.8 ± 0.6

[a] PHRR: peak of heat release rate; THR: total heat release; FPI: fire performance index, FPI = TTI/PHRR (TTI: time to ignition); FGR: fire growth rate, FGR = PHRR/T_{PHRR} (T_{PHRR}: time to PHRR); TSP: total smoke production; PSPR: peak of smoke production rate; AEHC: average of effective heat of combustion; and RW: residual weight at 500 s.

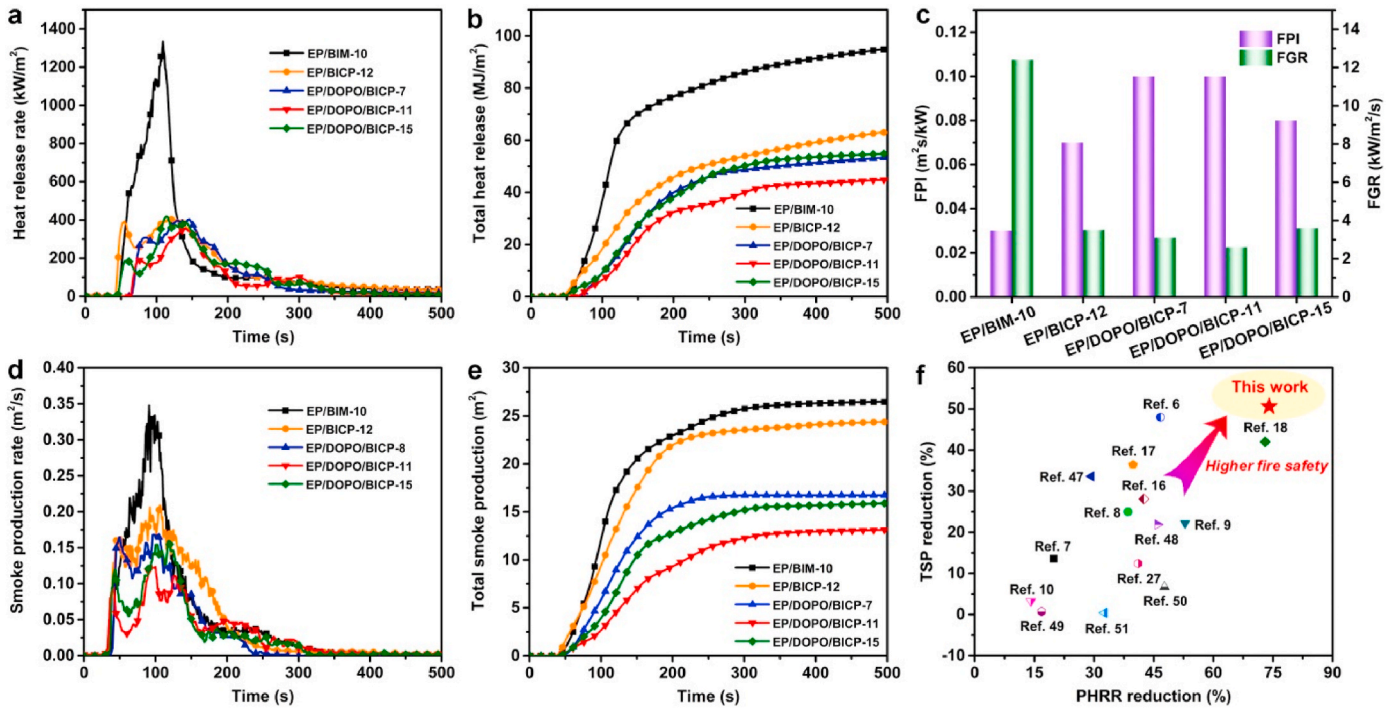

Fig. 3. (a) HRR curves, (b) THR curves, (c) FPI and FGR, (d) SPR curves, (e) TSP curves of EP sample and (f) PHRR and TSP reductions of EP/DOPO/BICP-11 sample in this work and other flame-retardant P-containing EP samples in previous researches.

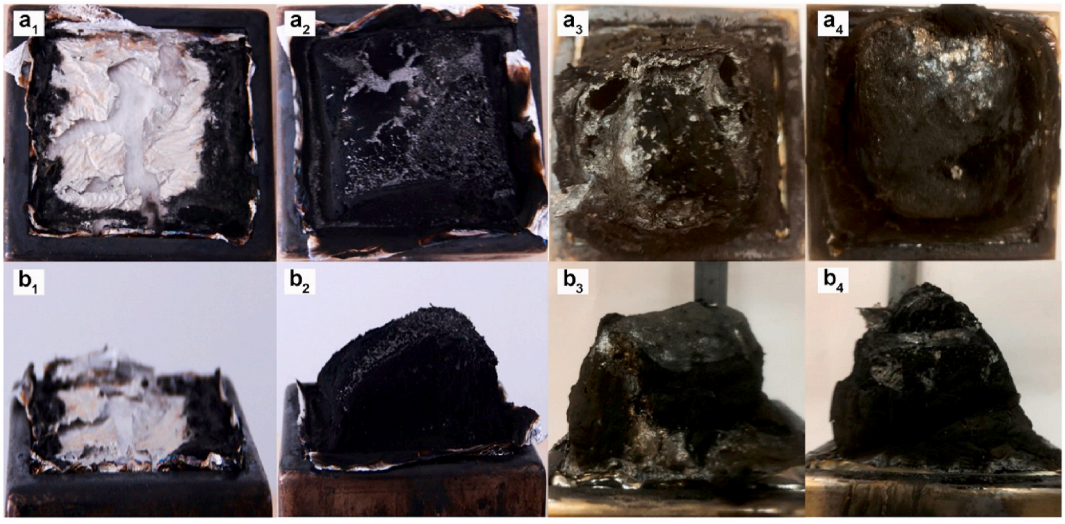

Fig. 4. Digital photographs of residual chars of EP/BIM-10 (a_1, b_1), EP/BICP-12 (a_2, b_2), EP/DOPO/BICP-11 (a_3, b_3) and EP/DOPO/BICP-15 (a_4, b_4) from top and side views.

the multiple flame-retardant mechanisms of EP/DOPO/BICP in the gas phase.

3.5. Morphology and chemical composition of char residues

To further elucidate the condensed-phase mechanism, the morphology and chemical composition of the char residues from cone calorimeter tests were performed. Obviously, without flame retardants, the char residue of EP/BIM-10 shows a broken and loose structure (see Fig. 6a_1), while that of EP/BICP-12 or EP/DOPO/BICP-11 is compact and continuous due to the introduction of P-containing groups (see Fig. 6b_1 and 6c_1). Such dense chars can effectively suppress the heat and mass transfer in the condensed phase, thus enhancing the flame retardance. Meanwhile, the EDS spectra of the char residues are shown in Fig. 6a_2-6c_2. The EDS results indicate that the main component of char residues is element carbon. A large amount of phosphorus is determined in the chars of both EP/BICP-12 and EP/DOPO/BICP-11, further indicating that such an intumescent and compact char layer is attributed to the catalytic charring effect of P-containing groups in the condensed phase. In addition, both P and O contents of the char for the EP/DOPO/BICP-11 are higher than those of the char from EP/BICP-12, implying that more phosphoric and polyphosphoric acids are generated during the combustion of EP/DOPO/BICP-11, further promoting the carbonization of the EP matrix [67,68].

The graphitization degrees of the chars of EP/BIM-10, EP/BICP-12 and EP/DOPO/BICP-11 were quantitatively evaluated by Raman

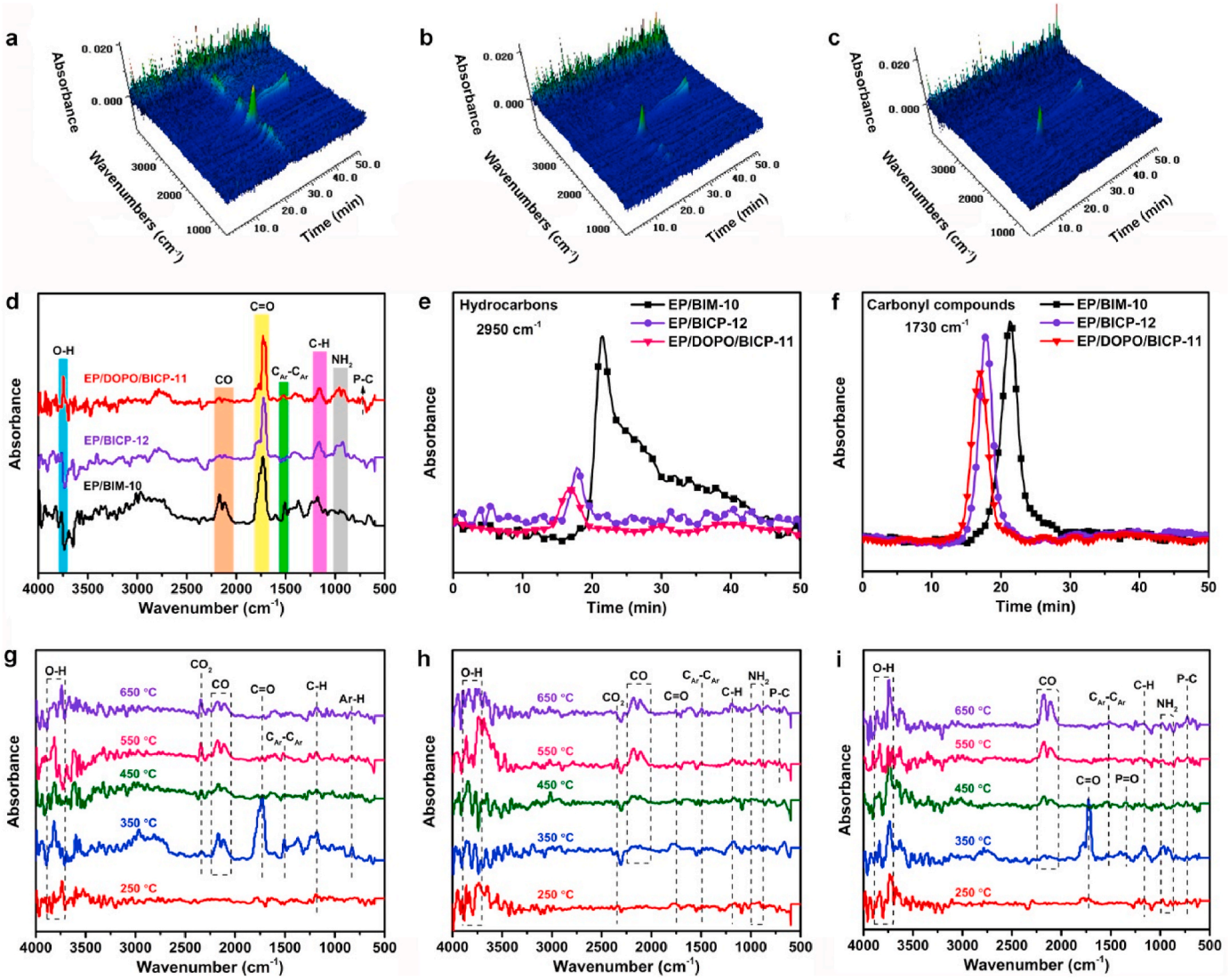

Fig. 5. 3D FTIR spectra of the pyrolysis products of (a) EP/BIM-10, (b) EP/BICP-12 and (c) EP/DOPO/BICP-11; (d) FTIR spectra of the pyrolysis products of EPs at the maximum gas release rate; the absorption *vs.* time curves of the peaks at (e) 2950 and (f) 1730 cm^{-1} of EPs; FTIR spectra of the pyrolysis products of (g) EP/BIM-10, (h) EP/BICP-12 and (i) EP/DOPO/BICP-11 at different temperatures.

spectroscopy. As shown in Fig. 6c_1-6c_3, all Raman spectra show D and G peaks centered at 1355 and 1582 cm^{-1}, respectively. The proportion of the intensity of D peak to G peak (I_D/I_G) can estimate the graphitization degree of char, and the lower the I_D/I_G value indicate the higher the graphitization degree [69,70]. The char of EP/DOPO/BICP-11 exhibits the minimum I_D/I_G value, manifesting the highest graphitization degree. The char layer with high graphitization degree is conducive to protecting the underlying matrix and suppressing the combustion, thus leading to enhanced flame retardancy.

3.6. Flame retardant mechanism

Given the above analyses, a possible flame-retardant mechanism of EP/DOPO/BICPs is proposed in Scheme 3. For phosphaphenanthrene groups, they decompose to release P-containing fragments (e.g., HPO and PO•) into the gaseous phase, which scavenge active O•, H• and HO• radicals generated by the degradation of epoxy matrix, thus interrupting the chain combustion reactions in the gas phase. Meanwhile, cyclotriphosphazene groups decompose to release NH_2 that exerts a diluting effect in the gaseous phase. In addition, cyclotriphosphazene groups cooperate with phosphaphenanthrene groups to promote the formation of an intumescent and compact P-rich char shield in the condensed phase, which inhibits the oxygen/heat-exchange and smoke release, thus bringing about a boost in flame retardancy and smoke suppression. In brief, the combination of phosphaphenanthrene and cyclotriphosphazene groups endows epoxy/imidazole system with great flame retardancy and smoke suppression.

4. Conclusions

In this work, we have rationally designed a fire-safe and tunable-temperature curable one-component EP/DOPO/BICP system. EP/DOPO/BICP-11 exhibits improved storage stability and a long shelf life of ~20 days. In addition, the DOPO serves as a switch that prompts BICP to release BIM *via* substitution reaction in initial curing stage, leading to reduced curing temperatures. Moreover, EP/DOPO/BICP system features superior flame retardancy and smoke suppression. For instance, EP/DOPO/BICP-11 exhibits a high LOI value of 38.3% and a UL-94 V-0 rating, with ~74.5% and ~50.6% reductions in PHRR and TSP. The remarkable enhancements in flame retardancy and smoke suppression are mainly due to the cooperation of cyclotriphosphazene and phosphaphenanthrene groups in both gas and condensed phases.

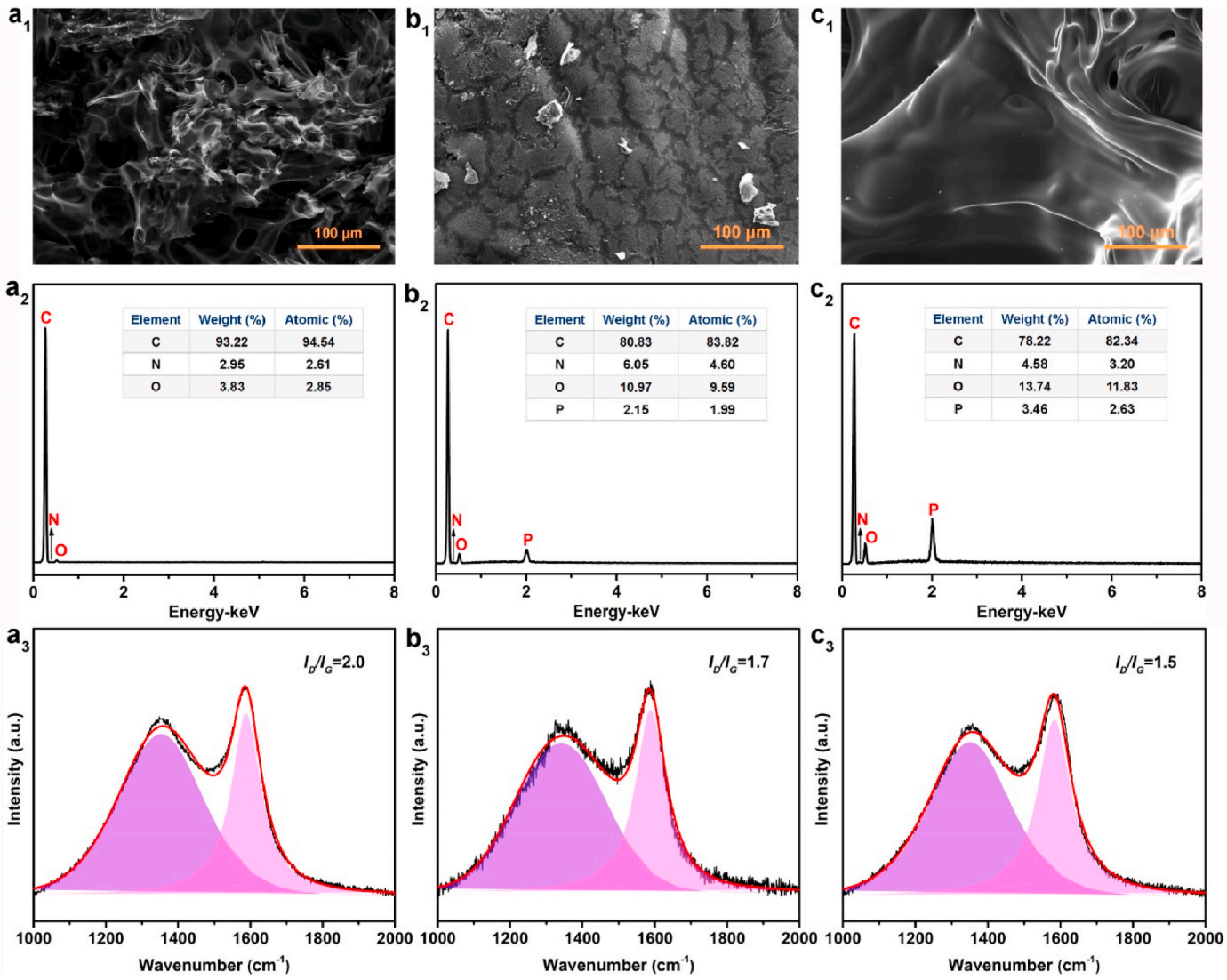

Fig. 6. The SEM images, EDS spectra and Raman spectra of the char residues of EP/BIM-10 (a_1, a_2, a_3), EP/BICP-12 (b_1, b_2, b_3) and EP/DOPO/BICP-11 (c_1, c_2, c_3) from cone calorimeter tests.

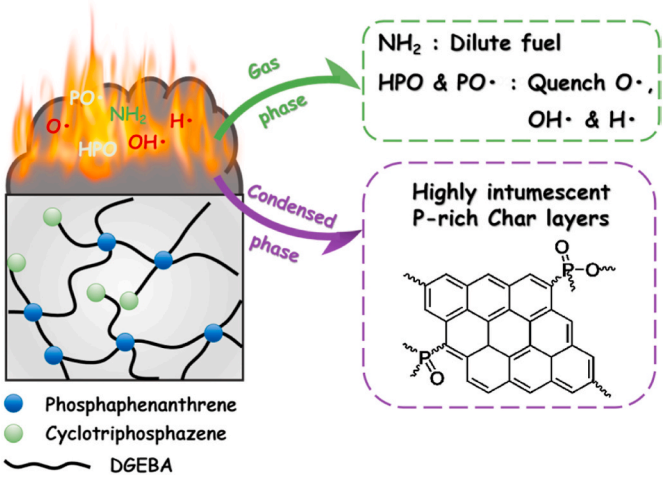

Scheme 3. Illustration of flame-retardant mechanism of EP/DOPO/BICPs.

This work offers a simple and scalable strategy for the design of switchable-temperature curable and rapid-curing one-component epoxy resins combining excellent flame retardancy and smoke suppression, thus expecting to satisfy the requirements of large-scale production.

CRediT authorship contribution statement

Shuang Yang: Conceptualization, Resources, Project administration, Funding acquisition. **Siqi Huo:** Investigation, Data curation, Formal analysis, Writing - original draft, preparation, Writing - review & editing. **Jun Wang:** Conceptualization, Resources, Project administration. **Bin Zhang:** Investigation, Data curation. **Jingsheng Wang:** Investigation, Data curation. **Shiya Ran:** Investigation, Formal analysis. **Zhengping Fang:** Investigation, Formal analysis, Supervision. **Pingan Song:** Writing - original draft, preparation, Supervision. **Hao Wang:** Supervision, Funding acquisition.

Declaration of competing interest

We declare that we do not have any commercial or associative interest that represents a conflict of interest in connection with the work submitted.

Acknowledges

This work was financially supported by the National Natural Science Foundation of China (No. 51803159, 51903193 and 51873196), and the Australian Research Council Discovery Project (No. DP190102992, FT190100188).

Appendix A. Supplementary data

Supplementary data to this article can be found online at https://doi.org/10.1016/j.compositesb.2020.108601.

References

[1] Shi Y, Liu C, Liu L, Fu L, Yu B, Lv Y, et al. Strengthening, toughing and thermally stable ultra-thin MXene nanosheets/polypropylene nanocomposites via nanoconfinement. Chem Eng J 2019;378:122267.
[2] Lazar ST, Kolibaba TJ, Grunlan JC. Flame-retardant surface treatments. Nat Rev Mater 2020;5(4):259–75.
[3] Nie S, Jin D, Xu Y, Han C, Dong X, Yang J-n. Effect of a flower-like nickel phyllosilicate-containing iron on the thermal stability and flame retardancy of epoxy resin. J Mater Res Technol 2020;9(5):10189–97.
[4] Xue Y, Shen M, Zeng S, Zhang W, Hao L, Yang L, et al. A novel strategy for enhancing the flame resistance, dynamic mechanical and the thermal degradation properties of epoxy nanocomposites. Mater Res Express 2019;6(12):125003.
[5] Fang F, Ran S, Fang Z, Song P, Wang H. Improved flame resistance and thermo-mechanical properties of epoxy resin nanocomposites from functionalized graphene oxide via self-assembly in water. Compos B Eng 2019;165:406–16.
[6] Yang G, Wu WH, Wang YH, Jiao YH, Lu LY, Qu HQ, et al. Synthesis of a novel phosphazene-based flame retardant with active amine groups and its application in reducing the fire hazard of Epoxy Resin. J Hazard Mater 2019;366:78–87.
[7] Zhao P, Rao W, Luo H, Wang L, Liu Y, Yu C. Novel organophosphorus compound with amine groups towards self-extinguishing epoxy resins at low loading. Mater Des 2020;193:108838.
[8] Zhao J, Dong X, Huang S, Tian X, Song L, Yu Q, et al. Performance comparison of flame retardant epoxy resins modified by DPO–PHE and DOPO–PHE. Polym Degrad Stabil 2018;156:89–99.
[9] Fang F, Huo S, Shen H, Ran S, Wang H, Song P, et al. A bio-based ionic complex with different oxidation states of phosphorus for reducing flammability and smoke release of epoxy resins. Compos Commun 2020;17:104–8.
[10] Xu Y-J, Shi X-H, Lu J-H, Qi M, Guo D-M, Chen L, et al. Novel phosphorus-containing imidazolium as hardener for epoxy resin aiming at controllable latent curing behavior and flame retardancy. Compos B Eng 2020;184:107673.
[11] Yang B, Mao Y, Zhang Y, Bian G, Zhang L, Wei Y, et al. A novel liquid imidazole-copper (II) complex as a thermal latent curing agent for epoxy resins. Polymer 2019;178:121586.
[12] Huo S, Yang S, Wang J, Cheng J, Zhang Q, Hu Y, et al. A liquid phosphaphenanthrene-derived imidazole for improved flame retardancy and smoke suppression of epoxy resin. ACS Appl Polym Mater 2020;2(8):3566–75.
[13] Kudo K, Furutani M, Arimitsu K. Imidazole derivatives with an intramolecular hydrogen bond as thermal latent curing agents for thermosetting resins. ACS Macro Lett 2015;4(10):1085–8.
[14] Yang S, Zhang Q, Hu Y, Ding G, Wang J, Huo S, et al. Synthesis of s-triazine based tri-imidazole derivatives and their application as thermal latent curing agents for epoxy resin. Mater Lett 2018;216:127–30.
[15] Arimitsu K, Fuse S, Kudo K, Furutani M. Imidazole derivatives as latent curing agents for epoxy thermosetting resins. Mater Lett 2015;161:408–10.
[16] Wang P, Xiao H, Duan C, Wen B, Li Z. Sulfathiazole derivative with phosphaphenanthrene group: synthesis, characterization and its high flame-retardant activity on epoxy resin. Polym Degrad Stabil 2020;173:109078.
[17] Ma W, Xu B, Shao L, Liu Y, Chen Y, Qian L. Synthesis of (1,4-methylenephenylphosphinic acid) piperazine and its application as a flame retardant in epoxy thermosets. Macromol Mater Eng 2019;304(12):1900419.
[18] Fang Y, Miao J, Yang X, Zhu Y, Wang G. Fabrication of polyphosphazene covalent triazine polymer with excellent flame retardancy and smoke suppression for epoxy resin. Chem Eng J 2020;385:123830.
[19] Zhu Z-M, Shang K, Wang L-X, Wang J-S. Synthesis of an effective bio-based flame-retardant curing agent and its application in epoxy resin: curing behavior, thermal stability and flame retardancy. Polym Degrad Stabil 2019;167:179–88.
[20] Huo S, Liu Z, Wang J. Thermal properties and flame retardancy of an intumescent flame-retarded epoxy system containing phosphaphenanthrene, triazine-trione and piperidine. J Therm Anal Calorim 2019;139(2):1099–110.
[21] Pourchet S, Sonnier R, Ben-Abdelkader M, Gaillard Y, Ruiz Q, Placet V, et al. New reactive isoeugenol based phosphate flame retardant: toward green epoxy resins. ACS Sustainable Chem Eng 2019;7(16):14074–88.
[22] Liang W-j, Zhao B, Zhao P-h, Zhang C-y, Liu Y-q. Bisphenol-S bridged penta (anilino)cyclotriphosphazene and its application in epoxy resins: synthesis, thermal degradation, and flame retardancy. Polym Degrad Stabil 2017;135:140–51.
[23] Qiu S, Zhou Y, Zhou X, Zhang T, Wang C, Yuen RKK, et al. Air-stable polyphosphazene-functionalized few-layer black phosphorene for flame retardancy of epoxy resins. Small 2019;15(10):1805175.
[24] Xu Y-J, Chen L, Rao W-H, Qi M, Guo D-M, Liao W, et al. Latent curing epoxy system with excellent thermal stability, flame retardance and dielectric property. Chem Eng J 2018;347:223–32.
[25] Huo S, Yang S, Wang J, Cheng J, Zhang Q, Hu Y, et al. A liquid phosphorus-containing imidazole derivative as flame-retardant curing agent for epoxy resin with enhanced thermal latency, mechanical, and flame-retardant performances. J Hazard Mater 2020;386:121984.
[26] Xu Y-J, Wang J, Tan Y, Qi M, Chen L, Wang Y-Z. A novel and feasible approach for one-pack flame-retardant epoxy resin with long pot life and fast curing. Chem Eng J 2018;337:30–9.
[27] Cheng J, Wang J, Yang S, Zhang Q, Huo S, Zhang Q, et al. Benzimidazolyl-substituted cyclotriphosphazene derivative as latent flame-retardant curing agent for one-component epoxy resin system with excellent comprehensive performance. Compos B Eng 2019;177:107440.
[28] Qiu S, Ma C, Wang X, Zhou X, Feng X, Yuen RK, et al. Melamine-containing polyphosphazene wrapped ammonium polyphosphate: a novel multifunctional organic-inorganic hybrid flame retardant. J Hazard Mater 2018;344:839–48.
[29] Qiu S, Wang X, Yu B, Feng X, Mu X, Yuen RK, et al. Flame-retardant-wrapped polyphosphazene nanotubes: a novel strategy for enhancing the flame retardancy and smoke toxicity suppression of epoxy resins. J Hazard Mater 2017;325:327–39.
[30] Zhang Q, Wang J, Yang S, Cheng J, Ding G, Huo S. Facile construction of one-component intrinsic flame-retardant epoxy resin system with fast curing ability using imidazole-blocked bismaleimide. Compos B Eng 2019;177:107380.
[31] Xu M-J, Xu G-R, Leng Y, Li B. Synthesis of a novel flame retardant based on cyclotriphosphazene and DOPO groups and its application in epoxy resins. Polym Degrad Stabil 2016;123:105–14.
[32] Jiang P, Gu X, Zhang S, Wu S, Zhao Q, Hu Z. Synthesis, characterization, and utilization of a novel phosphorus/nitrogen-containing flame retardant. Ind Eng Chem Res 2015;54(11):2974–82.
[33] Qian L, Ye L, Qiu Y, Qu S. Thermal degradation behavior of the compound containing phosphaphenanthrene and phosphazene groups and its flame retardant mechanism on epoxy resin. Polymer 2011;52(24):5486–93.
[34] Allcock HR, Fuller T. Synthesis and hydrolysis of hexakis (imidazolyl) cyclotriphosphazene. J Am Chem Soc 1981;103(9):2250–6.
[35] Ogueri KS, Allcock HR, Laurencin CT. Generational biodegradable and regenerative polyphosphazene polymers and their blends with poly (lactic-co-glycolic acid). Prog Polym Sci 2019;98.
[36] Wang Y, Zhang X, Li A, Li M. Intumescent flame retardant-derived P,N co-doped porous carbon as an efficient electrocatalyst for the oxygen reduction reaction. Chem Commun (Camb) 2015;51(79):14801–4.
[37] Wang CS, Lin CH. Synthesis and properties of phosphorus-containing epoxy resins by novel method. J Polym Sci, Part A: Polym Chem 1999;37(21):3903–9.
[38] Kudo K, Fuse S, Furutani M, Arimitsu K. Imidazole-type thermal latent curing agents with high miscibility for one-component epoxy thermosetting resins. J Polym Sci, Part A: Polym Chem 2016;54(17):2680–8.
[39] Chu F, Ma C, Zhang T, Xu Z, Mu X, Cai W, et al. Renewable vanillin-based flame retardant toughening agent with ultra-low phosphorus loading for the fabrication of high-performance epoxy thermoset. Compos B Eng 2020;190:107925.
[40] Tang S, Qian L, Liu X, Dong Y. Gas-phase flame-retardant effects of a bi-group compound based on phosphaphenanthrene and triazine-trione groups in epoxy resin. Polym Degrad Stabil 2016;133:350–7.
[41] Wen X, Liu Z, Li Z, Zhang J, Wang D-Y, Szymańska K, et al. Constructing multifunctional nanofiller with reactive interface in PLA/CB-g-DOPO composites for simultaneously improving flame retardancy, electrical conductivity and mechanical properties. Compos Sci Technol 2020;188:107988.
[42] Xue Y, Feng J, Huo S, Song P, Yu B, Liu L, et al. Polyphosphoramide-intercalated MXene for simultaneously enhancing thermal stability, flame retardancy and mechanical properties of polylactide. Chem Eng J 2020;397:125336.
[43] Huang G, Chen W, Wu T, Guo H, Fu C, Xue Y, et al. Multifunctional graphene-based nano-additives toward high-performance polymer nanocomposites with enhanced mechanical, thermal, flame retardancy and smoke suppressive properties. Chem Eng J 2020:127590.
[44] Yang S, Wang J, Huo S, Cheng L, Wang M. The synergistic effect of maleimide and phosphaphenanthrene groups on a reactive flame-retarded epoxy resin system. Polym Degrad Stabil 2015;115:63–9.
[45] Qian L, Qiu Y, Sun N, Xu M, Xu G, Xin F, et al. Pyrolysis route of a novel flame retardant constructed by phosphaphenanthrene and triazine-trione groups and its flame-retardant effect on epoxy resin. Polym Degrad Stabil 2014;107:98–105.
[46] Tawiah B, Yu B, Yuen ACY, Yuen RKK, Xin JH, Fei B. Thermal, crystalline and mechanical properties of flame retarded Poly(lactic acid) with a PBO-like small molecule - phenylphosphonic Bis(2-aminobenzothiazole). Polym Degrad Stabil 2019;163:76–86.
[47] Xu X, Dai J, Ma Z, Liu L, Zhang X, Liu H, et al. Manipulating interphase reactions for mechanically robust, flame-retardant and sustainable polylactide biocomposites. Compos B Eng 2020:107930.
[48] Anseeuw K, Delvau N, Burillo-Putze G, De Iaco F, Geldner G, Holmstrom P, et al. Cyanide poisoning by fire smoke inhalation: a European expert consensus. Eur J Emerg Med 2013;20(1):2–9.
[49] Xie W, Huang S, Tang D, Liu S, Zhao J. Synthesis of a furfural-based DOPO-containing co-curing agent for fire-safe epoxy resins. RSC Adv 2020;10(4):1956–65.
[50] Ma C, Qiu S, Yu B, Wang J, Wang C, Zeng W, et al. Economical and environment-friendly synthesis of a novel hyperbranched poly(aminomethylphosphine oxide-amine) as co-curing agent for simultaneous improvement of fire safety, glass transition temperature and toughness of epoxy resins. Chem Eng J 2017;322:618–31.

[51] Hu X, Yang H, Jiang Y, He H, Liu H, Huang H, et al. Facile synthesis of a novel transparent hyperbranched phosphorous/nitrogen-containing flame retardant and its application in reducing the fire hazard of epoxy resin. J Hazard Mater 2019;379:120793.
[52] Qiu Y, Qian L, Feng H, Jin S, Hao J. Toughening effect and flame-retardant behaviors of phosphaphenanthrene/phenylsiloxane bigroup macromolecules in epoxy thermoset. Macromolecules 2018;51(23):9992–10002.
[53] Liu X-F, Liu B-W, Luo X, Guo D-M, Zhong H-Y, Chen L, et al. A novel phosphorus-containing semi-aromatic polyester toward flame retardancy and enhanced mechanical properties of epoxy resin. Chem Eng J 2020;380:122471.
[54] Peng C, Chen T, Zeng B, Chen G, Yuan C, Xu Y, et al. Anderson-type polyoxometalate-based hybrid with high flame retardant efficiency for the preparation of multifunctional epoxy resin nanocomposites. Compos B Eng 2020;186:107780.
[55] Zhu M, Liu L, Wang Z. Mesoporous silica via self-assembly of nano zinc amino-tris-(methylenephosphonate) exhibiting reduced fire hazards and improved impact toughness in epoxy resin. J Hazard Mater 2020;392:122343.
[56] Yang S, Wang J, Huo S, Wang M, Cheng L. Synthesis of a phosphorus/nitrogen-containing additive with multifunctional groups and its flame-retardant effect in epoxy resin. Ind Eng Chem Res 2015;54(32):7777–86.
[57] Yang H, Yu B, Xu X, Bourbigot S, Wang H, Song P. Lignin-derived bio-based flame retardants toward high-performance sustainable polymeric materials. Green Chem 2020;22(7):2129–61.
[58] Huo S, Liu Z, Li C, Wang X, Cai H, Wang J. Synthesis of a phosphaphenanthrene/benzimidazole-based curing agent and its application in flame-retardant epoxy resin. Polym Degrad Stabil 2019;163:100–9.
[59] Feng J, Xu X, Xu Z, Xie H, Song P, Li L, et al. One-Pot, solvent-and catalyst-free synthesis of polyphosphoramide as an eco-benign and effective flame retardant for poly (lactic acid). ACS Sustainable Chem Eng 2020;8(44):16612–23.
[60] Chen S, Ai L, Zhang T, Liu P, Liu W, Pan Y, et al. Synthesis and application of a triazine derivative containing boron as flame retardant in epoxy resins. Arab J Chem 2020;13(1):2982–94.
[61] Yuan Y, Yu B, Shi Y, Mao L, Xie J, Pan H, et al. Insight into hyper-branched aluminum phosphonate in combination with multiple phosphorus synergies for fire-safe epoxy resin composites. Polymers 2020;12(1).
[62] Xue Y, Shen M, Zheng Y, Tao W, Han Y, Li W, et al. One-pot scalable fabrication of an oligomeric phosphoramide towards high-performance flame retardant polylactic acid with a submicron-grained structure. Compos B Eng 2020;183:107695.
[63] Shao Z, Yue W, Piao M, Ma J, Lv X, Wang D, et al. An excellent intrinsic transparent epoxy resin with high flame retardancy: synthesis, characterization, and properties. Macromol Mater Eng 2019;304(10):1900254.
[64] He W, Song P, Yu B, Fang Z, Wang H. Flame retardant polymeric nanocomposites through the combination of nanomaterials and conventional flame retardants. Prog Mater Sci 2020;114:100687.
[65] Yang H, Yu B, Song P, Maluk C, Wang H. Surface-coating engineering for flame retardant flexible polyurethane foams: a critical review. Compos B Eng 2019;176:107185.
[66] Qiu S, Zou B, Zhang T, Ren X, Yu B, Zhou Y, et al. Integrated effect of NH_2-functionalized/triazine based covalent organic framework black phosphorus on reducing fire hazards of epoxy nanocomposites. Chem Eng J 2020;401:126058.
[67] Zhang Q, Yang S, Wang J, Cheng J, Zhang Q, Ding G, et al. A DOPO based reactive flame retardant constructed by multiple heteroaromatic groups and its application on epoxy resin: curing behavior, thermal degradation and flame retardancy. Polym Degrad Stabil 2019;167:10–20.
[68] Liu L, Xu Y, Li S, Xu M, He Y, Shi Z, et al. A novel strategy for simultaneously improving the fire safety, water resistance and compatibility of thermoplastic polyurethane composites through the construction of biomimetic hydrophobic structure of intumescent flame retardant synergistic system. Compos B Eng 2019;176:107218.
[69] Zhang Y, Xiong Z, Ge H, Ni L, Zhang T, Huo S, et al. Core–shell bioderived flame retardants based on chitosan/alginate coated ammonia polyphosphate for enhancing flame retardancy of polylactic acid. ACS Sustainable Chem Eng 2020;8(16):6402–12.
[70] Xu Z, Duan L, Hou Y, Chu F, Jiang S, Hu W, et al. The influence of carbon-encapsulated transition metal oxide microparticles on reducing toxic gases release and smoke suppression of rigid polyurethane foam composites. Compos Part A Appl Sci Manuf 2020;131:105815.